Semi-Automated Road Detection From High Resolution Satellite Images by Directional Morphological Enhancement and Segmentation Techniques

D. Chaudhuri, N. K. Kushwaha, and A. Samal

***Abstract*—Extraction of map objects such roads, rivers and buildings from high resolution satellite imagery is an important task in many civilian and military applications. We present a semi-automatic approach for road detection that achieves high accuracy and efficiency. This method exploits the properties of road segments to develop customized operators to accurately derive the road segments. The customized operators include directional morphological enhancement, directional segmentation and thinning. We have systematically evaluated the algorithm on a variety of images from IKONOS, QuickBird, CARTOSAT-2A satellites and carefully compared it with the techniques presented in literature. The results demonstrate that the algorithm proposed is both accurate and efficient.**

***Index Terms*—Enhancement, morphology, remote sensing, resolution, road detection, segmentation.**

I. Introduction

EXTRACTION of features from satellite/aerial imagery is an important task in many applications that rely on geographic information systems (GIS). Recognition of roads is critical since they form an important GIS layer in significant civilian and military applications including navigation or location aware systems and emergency planning systems for evacuation and fire response. Automated road extraction can save both time and labor to build and update the road spatial database in such applications. However, fully automated algorithms to recognize them for applications where accuracy is critical are not currently available. Use of high resolution imagery facilitates greater accuracy, but in turn increases the computational and problem complexity due to noise and artifacts. We present an accurate semi-automated approach to recognize roads from high-resolution satellite imagery.

A rich body of literature exists in automated road extraction [31]. Xiong [1] grouped the methods into five categories: (a) ridge finding, (b) heuristic reasoning, (c) dynamic programming, (d) statistical inference, and (e) map matching. Road appears as ridges or valleys of gray value function of an image. *Ridge finding* methods use edge operators to derive edge magnitude and direction, followed by thresholding and thinning to obtain ridge pixels [2], [3]. Ridge points are then linked to produce the road segments. *Heuristic reasoning* methods use prior knowledge in the form of pre-set rules about road characteristics to identify road segments [4], [5]. *Dynamic programming* methods model roads with a set of mathematical equations on the derivatives of gray values and select characteristics of roads and use them to solve the optimization problem [6], [7]. *Statistical inference* methods model linear features as a Markov point process or a geometric-stochastic model on the road width, direction, intensity and background intensity, and use maximum a *posteriori* probability to estimate the road network [8], [9], [23]. *Map matching* methods use existing road maps as a starting point to update the road network using a two-step approach. First, a map-image algorithm is employed to match the roads on the map to the image. New roads are then searched based on the assumption that they are connected to existing roads [10].

Most of the research in road extraction from high resolution imagery has focused on IKONOS, QuickBird and CARTOSAT-2A satellites [12]–[14]. Among the recognition techniques, knowledge-based approaches and morphology-based methods have been widely used [15]–[19], [24], [26]. Hu and Tao [11] suggested a hierarchical grouping strategy to automatically extract the road centerlines from high resolution satellite imagery. Ahmed and Rahman have proposed a two-step approach for identification of road intersections of urban areas [26].A number of methods to extract roads from multi-spectral and panchromatic images have been proposed [13], [25], [27], [28]. Zhang and Coulorigner proposed a fuzzy logic based classifier to road identification for high resolution multi-spectral imagery [25]. Doucette *et al.* proposed a methodology for fully automated road extraction that exploits spectral content from high resolution multispectral images [27]. Ziems *et al.* proposed an approach for the extraction of roads in open landscape regions from IKONOS multispectral imagery [28] using a line-based approach. Ünsalan and Boyer have described an approach to detect house and road from multispectral images [30] using NDVI to detect human activity and K-means clustering with spatial coherence (KMC-SC) to group pixels.

Manuscript received July 12, 2011; revised December 14, 2011 and March 14, 2012; accepted April 07, 2012. Date of publication June 28, 2012; date of current version November 14, 2012.

D. Chaudhuri and N. K. Kushwaha are with the IAC, DEAL, Raipur Road, Dehradun-248001, Uttarakhand, India (corresponding author, e-mail: deba_chaudhuri@yahoo.co.in)

A. Samal is with the Department of Computer Science and Engineering, University of Nebraska-Lincoln, Lincoln, NE 68588 USA.

Color versions of one or more of the figures in this paper are available online at http://ieeexplore.ieee.org.

Digital Object Identifier 10.1109/JSTARS.2012.2199085

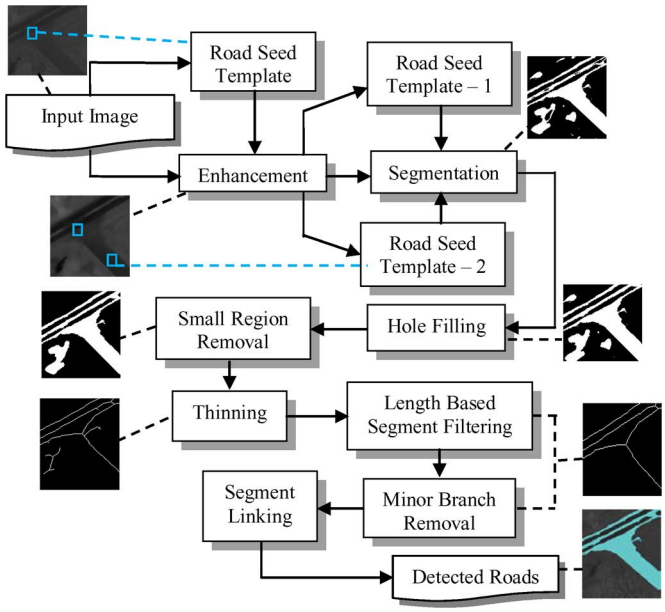

Fig. 1. Flowchart of the proposed road detection algorithm.

This paper presents a method to extract roads from high resolution panchromatic images using a multi-step approach. Other contributions of the paper include an extensive evaluation on a variety of satellite imagery and a uniquely detailed comparison with many algorithms proposed in literature.

II. Road Detection Algorithm

The proposed algorithm uses a *semi-automatic* approach for road detection with focus on accuracy and efficiency. Fig. 1 shows the flowchart of the algorithm. The details of each step are presented next in this section.

A. Image Enhancement

The goal of the enhancement step is to improve the visual effect in the image to facilitate geographic image interpretation and to improve the contrast between the target and the background for high level processing. A good enhancement operator will significantly reduce (or increase) the brightness of dark (or bright) road structures in the original image but has no effect on non-target pixels. We propose an enhancement technique based directional morphological operations: erosion, dilation, opening and closing.

The proposed enhancement technique is based on the local morphological operations that are directional in nature. To enhance the road structures in the image, we use a customized 5 $\times$ 5 structuring element to serve as a road seed template. Both enhancement and segmentation techniques are more effective with a smaller window. Using a larger window would pose difficulty in these two steps at the boundary of the roads. As shown in Fig. 2, only four directions: horizontal, vertical and left and right diagonals are used. This provides a good balance between computational efficiency and enhancing the road structures.

Given an image f, we define the directional window at a location (x, y), $f_d(x, y)$, is defined by the five pixels along the direction d (1, 2, 3 or 4) (See Fig. 2) centered around location (x, y). Similarly, S_d is defined as the five pixels of the structuring element along the direction d (1, 2, 3 or 4).

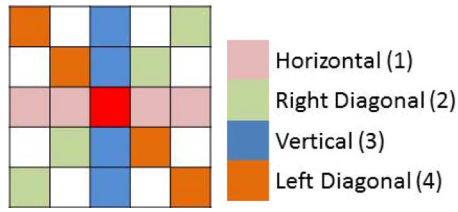

Fig. 2. Directions for morphological enhancement.

Enhancement Technique: Since opening suppresses bright regions smaller than the special structuring element, and closing suppresses dark regions, they are often used in combination as *morphological filters* for image smoothing and noise removal. The proposed enhancement technique is a combination of opening and closing operations using the same structuring element along the homogeneous direction with respect to the image and the road template. Steps in the enhancement technique are described below.

We first apply the erosion operator directionally for the whole image. Then the dilation operator is applied to the eroded image. Finally, the two operators are applied in reverse order (dilation followed by erosion). The approach of using the morphological operations in this manner is called *alternating sequential filtering*. There are two main motivations for the proposed enhancement technique. A morphological filter consisting of opening followed by closing can eliminate noise that manifests as randomly placed bright elements in a dark background and or as dark elements in a bright background. Since a road has a definite direction, the proposed enhancement technique is based on directional morphological filtering using the road template (structuring element). Most of the window based spatial filters consider target and non-target pixels especially in the border region and as a result the border region is distorted. In contrast, the proposed enhancement algorithm enhances in the direction in which the structure is homogeneous and as a result the border region is not distorted. Hence, the target features can be isolated from the background.

Fig. 3(a) shows an IKONOS image at 1 m resolution with white road structures. Our goal in this step is to enhance the white linear structures and remove the noise. Fig. 3(b) shows the result of the opening operation with a 5 $\times$ 5 structuring element. Fig. 3(c) shows the result of only closing the original image with the same structuring element. Fig. 3(d) shows the enhanced image using our proposed algorithm. As expected, this sequence shows that the enhancement using the proposed technique is effective.

for each pixel (x, y) in the image f

1. Compute the *mean gray* value, $\overline{\mu}_d(x, y) = (1/5)\sum_{i=1}^{4} |f_d(x, y)[i] - S_d[i]|$, $d = 1, \ldots, 4$
2. Compute the *standard deviation*, $\sigma_d(x, y) = \sqrt{(1/5)\sum_{i=1}^{5}(f_d(x, y)[i] - S_d[i] - \overline{\mu}_d(x, y)[i])^2}$, $d = 1, \ldots, 4$.
3. Find the direction d_{min} for which σ_d, $d = 1, \ldots, 4$ is minimum.

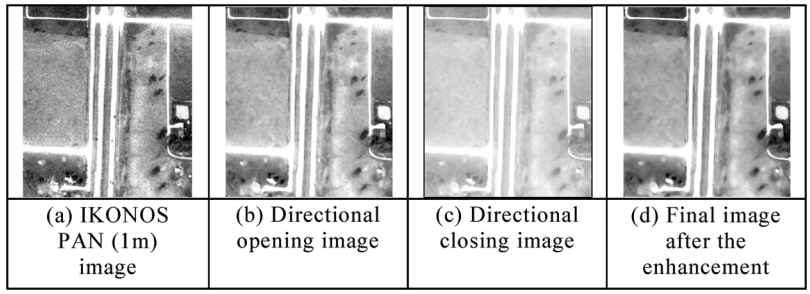

Fig. 3. Performance of the enhancement operation. (a) Original IKONOS PAN image, (b) directional opening image, (c) directional closing image and (d) image by proposed enhancement technique.

4. Perform gray level erosion at (x, y) using by the structuring element along the direction d_{min}.

Apply the contrast stretching with a range of [0, 255] to derive an intermediate image $g(x, y)$.

for each pixel (x, y) in the image g

5. Compute the *mean gray* value, $\overline{\mu}_d(x, y) = (1/5)\sum_{i=1}^{5} |g_d(x, y)[i] + S_d[i]|$, $d = 1, \ldots, 4$
6. Compute the *standard deviation*,

$$\sigma_d(x, y) = \sqrt{(1/5)\sum_{i=1}^{5}(g_d(x, y)[i] + S_d[i] - \overline{\mu}_d(x, y)[i])^2},$$

$d = 1, \ldots, 4$.

7. Find the direction d_{min} for which σ_d, $d = 1, \ldots, 4$ is minimum.
8. Perform gray level dilation at (x, y) using by the structuring element along the direction d_{min}.

Apply the contrast stretching with a range of [0, 255] to derive an intermediate image $h(x, y)$.

Repeat the above operations in reverse order (i.e. dilation followed by erosion).

B. Segmentation

The algorithm to efficiently isolate linear regions (roads) in the enhanced image is based on supervised directional homogeneity using Chaudhuri's metric [20]. Two carefully chosen 5×5 road seed templates from the enhanced image serve as the representatives. Line segments corresponding to road structures have definite directions, but due to discrete nature of the image, the directions of small-elongated objects are difficult to estimate. The proposed segmentation technique depends on the homogeneity with respect to the two road seed templates in different directions. Since looking for pixels in all directions can be expensive, we only consider a small set of directions. Our experiments showed that considering only eight directions (shown in Fig. 4) provides a good balance between computational efficiency and accurate extraction of road pixels.

In our segmentation step, we compare the image sections to the templates. Using Euclidean distance in high dimensional space is both computationally expensive and unstable. We therefore, use Chaudhuri's metric [20] which is close to Euclidean

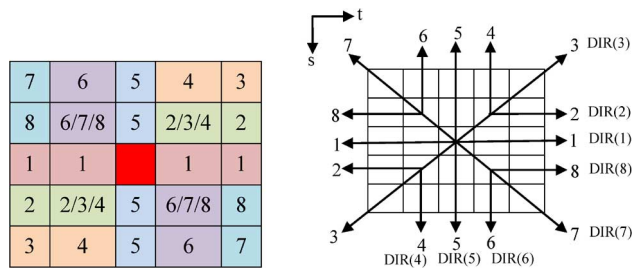

Fig. 4. Template directions for local homogeneity parameter calculation for segmentation.

distance and yet requires significantly less computational effort. Given two n-dimensional points, $X = (x_1, x_2, \ldots, x_n)$ and $Y = (y_1, y_2, \ldots, y_n)$, let $|x_i - y_i|$ be the maximum for $i = i_0$; the Chaudhuri's distance (d_{Ch}) is defined as

$$d_{Ch}(X, Y) = |X_{i_0} - Y_{i_0}| + \frac{1}{n - \lfloor \frac{n-2}{2} \rfloor} \sum_{\substack{i=1 \\ i \neq i_0}}^{n} |x_i - y_i| \quad (1)$$

where $\lfloor a \rfloor$ is the floor of "a", i.e. the largest integer $\leq a$.

The segmentation algorithm exploits the property that road structures are nearly homogeneous along a particular direction. So, the proposed segmentation algorithm operates with directional 5×5 windows. Along a given direction, we extract the 5 pixels from the image $[f_1, f_2, f_3, f_4, f_5]$, and for the two road seed templates, $[u_1, u_2, u_3, u_4, u_5]$ and $[v_1, v_2, v_3, v_4, v_5]$ as shown in Fig. 5. After the alignment of the pixels, we compute the distance between the image and the two templates. Similarly, we compute the distances for the pixel f_3 along 8 directions shown in Fig. 4.

Segmentation () {

for each pixel (i, j) {

$d_{final} = 0$;

for $(p = 1, \ldots, 8)$ {

$\mathrm{V}_{\mathrm{image}} = [f_1, f_2, f_3, f_4, f_5]$ = image vector for (i, j)-pixel along direction p;

$\mathrm{V}_{\mathrm{template-1}} = [u_1, u_2, u_3, u_4, u_5]$ first template vector along direction p;

$\mathrm{V}_{\mathrm{template-2}} = [v_1, v_2, v_3, v_4, v_5]$ second template vector along direction p;

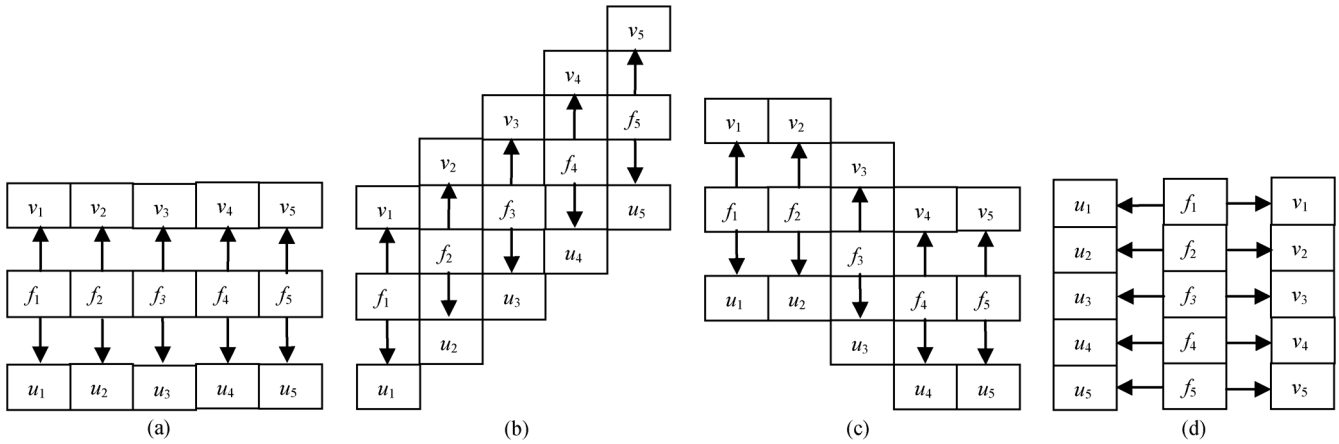

Fig. 5. Metric operation for central pixel f_3 by two templates along: (a) horizontal direction (1), (b) diagonal direction (3), (c) off-diagonal direction (8) and (d) vertical direction (5).

$$d_1 = d_{Ch}(\mathrm{V}_{\mathrm{image}}, \mathrm{V}_{\mathrm{template}-1});$$
$$d_2 = d_{Ch}(\mathrm{V}_{\mathrm{image}}, \mathrm{V}_{\mathrm{template}-2});$$
$$d_p = \min(d_1, d_2);$$

}

$$d_{final} = \min_{p=1.8}(d_p);$$

if $(d_{final} > T_{Seg})$ image $(i, j) = 0$;

else image $(i, j) = 1$;

}

}

The segmentation algorithm depends on a pre-defined threshold T_{Seg}, called the *homogeneity parameter*, which is sensitive to the separation of road and non-road pixels. Through extensive experimentation we have determined value of T_{Seg} between 25 and 30 gives the best results.

C. Hole Filling

Some regions identified after segmentation have holes due to noise. To overcome this problem of closing the non-road regions (crossing circles) in roundabouts (Fig. 6), we propose a simple and efficient algorithm. The segmented image is a binary image with road pixels labeled as 1's and non-road pixels as 0's. For small hole filling, we first invert the segmented image. We search all regions in non-road image and compute the areas by a recursive scanning method proposed in [21]. We then delete the small regions and invert this image. This results in an image which has no small holes with road pixels as "1" and non-road pixels as "0".

D. Area Based Filtering

Small regions that do not belong to any road are distributed all over the image. These regions are not of interest when the focus is on road extraction. Therefore, they are removed by a simple filtering technique on the basis of their area, i.e. regions whose area is less than a threshold are eliminated from further processing. Since we are interested in high resolution imagery, we have experimentally determined that a threshold (A^T) of 200 pixels is optimal.

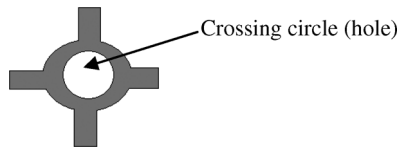

Fig. 6. Hole formation due to the situation of crossing.

E. Length Based Filtering

A linear representation facilitates both removal of non-linear regions and linking of linear regions that may have become disconnected in previous steps. In our implementation, we have used a well-known thinning algorithm described in [22]. We then remove two kinds of unwanted linear segments to improve the linear representation of the roads in the image.

Category 1: Regions corresponding to linear structures whose length (counted as number of pixels) is less than the minimum threshold (L^T) are first eliminated. We then remove the branches in the thinned image using an approach described in Section II-F. The basic idea is that small non-road linear elements are connected to the main road skeleton at one end and are not connected at the other end. The length of these elements is significantly less in comparison with the main road. So, we first find the main road structures and then use the branch removal process to eliminate minor linear regions. The optimal value of the threshold L^T was experimentally determined to be 10 pixels.

Category 2: The goal here is to eliminate long linear structures that are isolated. After minor branch removal, we determine the end pixels of the thinned version of the regions. Next, we try to find out the presence of any other thinned region within a specific neighborhood of the thinned version of a region. In order to make this efficient we identify the neighbors in a rectangular region as defined below.

We first find the two end pixels of linear representation of a region. Then find the $x_{\min}$, $x_{\max}$, $y_{\min}$ and $y_{\max}$ of these two end pixels. Length and width of the rectangular neighborhood is determined as $(x_{\max} - x_{\min} + 2R^T)$ and $(y_{\max} - y_{\min} + 2R^T)$

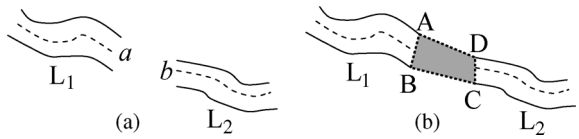

Fig. 7. Region based Linking procedure. (a) Two disconnected roads and (b) region based linking of two roads.

where *region searching parameter*, R^T is a predefined constant. The optimal constant value R^T was determined experimentally to be 25. For each region we determine if there are other regions in its rectangular neighborhood. Regions that have no other neighbors in the neighborhood are eliminated.

F. Minor Branch Removal

Many small non-road linear structures are associated with the main road skeleton. These are characterized by being connected to the main road at one end and free at the other. The lengths of these structures are significantly smaller in comparison with the length of the main road. These minor processes manifest as small branches in the thinned image. To accurately determine the main road, these small unwanted branches must be removed. Using an 8-neighborhood, we classify all the foreground pixels into *leaf*, *intermediate* or *junction* nodes. Pixels with one, two and three or more foreground neighbors are called leaf, intermediate and junction nodes, respectively. We identify the lengths of different segments in the thinned image by following pixels from the leaf nodes via intermediate nodes to the junction nodes. Branches that are shorter than a predefined threshold Len^T are removed. In our experiments, we have determined a $Len^T = 150$ to be optimal.

G. Segment Linking

At this stage there may exist some discontinuity between the thinned road linear features due to noise. So, we use a linking procedure to connect them based on their relative orientation and distances. Let a and b are two end pixels and the corresponding directions near the end be $\overline{a}$ and $\overline{b}$ (see Fig. 7). Also, let the direction from a and b be $\overline{c}$. We join the two segments corresponding to a and b by straight line if and only if (a) angle between $\overline{a}$ and $-\overline{b}$ is small, (b) angle between $\overline{a}$ and $\overline{c}$ is small, (c) angle between $\overline{c}$ and $-\overline{b}$ is small and (d) the distance between a and b (say, γ) is small.

For (a), (b) and (c) above the threshold for the angle is kept at the value 15°. The distance in (d) is used in a relative form. So, the condition (d) is satisfied if the ratio of the distance between a and b and the length of smaller segments corresponding to a and b (say, ζ) is less than a threshold, say Γ. The value of Γ is kept at 1.0.

Once two segments to be merged are identified, we locate the pixels that need to be mapped to road pixels. Since road structures are regions (not lines) the linked portion will also be a region. Fig. 7 illustrates how the linked portion region is determined. In Fig. 7, L_1 and L_2 are two road linear structures and their thinned linear structures are marked as dotted lines. Here a and b are the end points of the two segments and the thinned linear structures of L_1 and L_2 satisfy the above four conditions for linking at a and b. We find the points A and B for segment L_1 and C and D for segment L_2. We then join the polygon ADCB to the two segments L_1 and L_2 to derive a continuous linear structure.

III. Experimental Results and Discussions

In this paper, we evaluate the performance of our approach with scenes obtained from IKONOS and CARTOSAT-2A panchromatic imageries. We have also compared the results from the proposed algorithm with other algorithms in literature using IKONOS, QuickBird and Aerial images. Fig. 8(a) shows an original CARTOSAT-2A panchromatic image of size 512 $\times$ 512. The 5 $\times$ 5 road seed templates used for enhancement are also shown in Fig. 8(a). The enhanced image using the proposed enhancement technique is shown in Fig. 8(b). It is clear that the road structures in Fig. 8(b) are enhanced in comparison to the original road structures in Fig. 8(a). Two 5 $\times$ 5 road seed templates for segmentation are also shown. Fig. 8(c) shows the image after segmentation. The result shows that the road structures are accurately preserved. However, as expected holes are present in the segmented regions. Fig. 8(d) shows the image after the hole filling operation. The image after removal of smaller regions using area based filtering is shown in Fig. 8(e). Fig. 8(f) shows the thinned image. The result shows the presence of many small curvilinear features associated with main road. Such branches are removed from the main road by the proposed branch removal operation. Fig. 8(g) and Fig. 8(h) show the image after the removal of two categories of length based filtering. As expected smaller spurs are removed in Fig. 8(g) and isolated branches are removed in Fig. 8(h). Fig. 8(i) shows the final result with only the road structures.

Fig. 9 shows the effectiveness of our algorithm and compares our results with the algorithm proposed by Wang *et al.* [13] using IKONOS imagery. As can be seen from the images, our algorithm is able to extract a large road subnetwork (lower left) that the algorithm by Wang *et al.* [13] misses. Fig. 9(d) shows the detected roads using ERDAS IMAGINE OBJECTIVE Software after fixing 14 parameters. Clearly, the roads obtained using the proposed algorithm are more accurate than those generated by ERDAS IMAGINE OBJECTIVE Software [29].

Fig. 10 shows the performance of our algorithm for IKONOS imagery. One more panchromatic image from IKONOS satellite of size 331 $\times$ 369 is shown in Fig. 10(a). In contrast to the materials used in the previous images, the road structures here are white. The proposed algorithm accurately detects these types of roads as are shown in Fig. 10(b). As expected, the results from IKONOS images are more accurate since they have higher spatial resolution.

Fig. 11 shows the roads extracted by our algorithm from QuickBird satellite images of size 510 $\times$ 513. We have compared our results with the algorithm proposed by Ahmed and Rahman [26]. It is clear from the results that while algorithm by Ahmed and Rahman detects all the roads in the image, it detects many non-road features (e.g. buildings) as road features

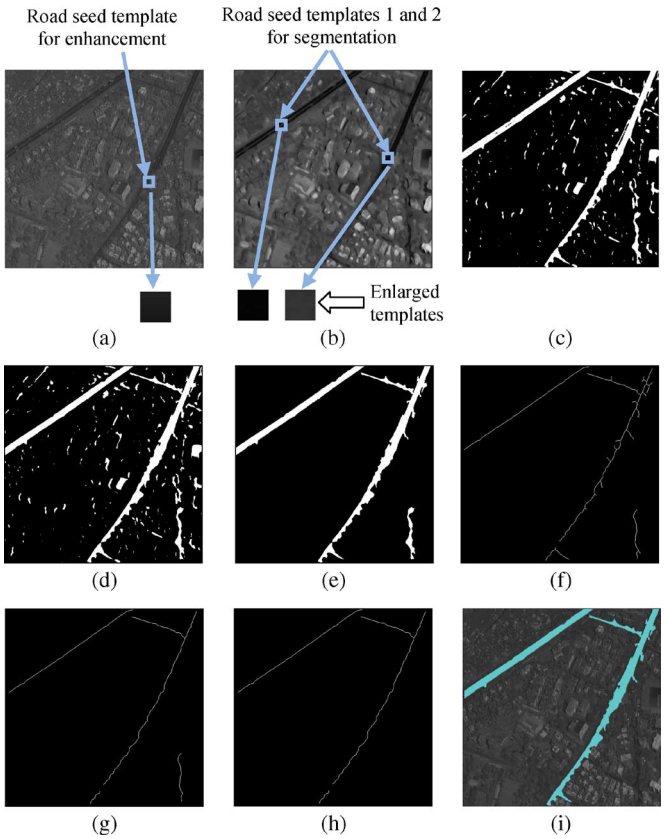

Fig. 8. Results with a CARTOSAT-2A PAN image. (a) Original image, (b) enhanced image (c) segmented image (d) hole-filled image, (e) image after removal of small regions, (f) thinned image, (g) image after removal of branches (Category 1), (h) image after removal of branches (Category 2),and (i) final detected roads.

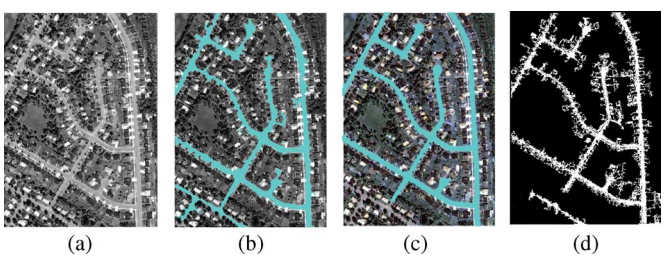

Fig. 9. Results for IKONOS satellite PAN image of ground resolution 1 × 1 m. (a) Original image, (b) detected roads by the proposed algorithm, (c) detected road by using Wang *et al* [13] algorithm and (d) detected road by ERDAS IMAGINE OBJECTIVE Software [29].

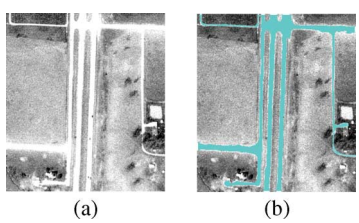

Fig. 10. Results for IKONOS satellite PAN image of ground resolution 1 × 1 m. (a) Original image with white road structures and (b) detected roads.

as well. The proposed algorithm detects all the roads perfectly without any false alarm.

Finally, Fig. 12 compares the performance of our algorithm with that of Ünsalan and Boyer [30] using a 455 × 454 IKONOS satellite image. The algorithm proposed by Ünsalan and Boyer (Fig. 12(b)) misses two large road segments (shown in blue). In contrast, the proposed algorithm is able to completely detect one of them (in the middle) and recognizes a large part of the other one (in the top part of the image) as shown in Fig. 12(c).

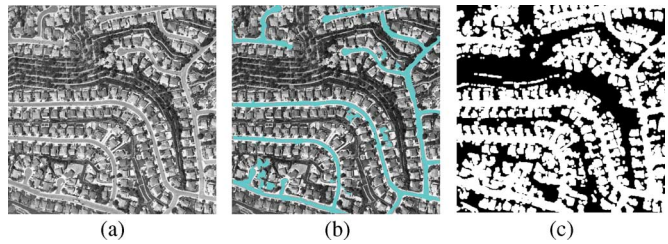

Fig. 11. QuickBird satellite converted grayscale image of ground resolution 2.44 m × 2.44 m. (a) Original grayscale image, (b) detected roads by the proposed algorithm and (c) detected road by using Ahmed and Rahman algorithm [26].

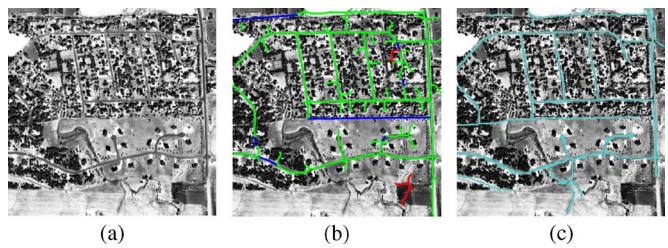

Fig. 12. The South Dakota image: (a) panchromatic image, (b) detected roads by Ünsalan and Boyer [30] method in which green: correct road, Blue: miss road and red: false alarm and (c) detected road by the proposed algorithm.

Several observations can be made on the basis of extensive performance evaluation of the proposed algorithm. We have compared the algorithm with other algorithms proposed in literature. We also have used different types of images in our comparison including IKONOS, CARTOSAT-2A, QuickBird and Arial panchromatic images. Most of main road segments are recognized by the proposed algorithm. Furthermore, the performance of the proposed algorithm is superior to others in both completeness and accuracy. The roads detected from IKONOS imagery are more accurate than those from CARTOSAT-2A images. It is because the CARTOSAT-2A images have lower resolution and thin road segments (less than 5 pixels wide) are not accurately recognized. Some of the thin segments can be recognized by using an approach described in [7]. Overall, the experimental analysis demonstrates the accuracy and efficiency of our proposed algorithm.

IV. Summary

We have presented a method to extract roads from high resolution panchromatic remotely sensed imagery. There are many civilian, commercial, and military applications for this problem including the determination of existence of roads after a natural or man-made disaster. The approach exploits both the spectral and spatial properties of roads using a multi-step approach. The main steps in our algorithm are: road enhancement, road segmentation, hole filling, small region filtering, length based region filtering, small branch removal method and road segment linking. The proposed algorithm was evaluated using IKONOS,

CARTOSAT-2A, QuickBird and Arial panchromatic images. The results demonstrate that the algorithm is highly accurate.

REFERENCES

[1] D. Xiong, "Automated road network extraction from high resolution images," NCRST—H White Papers [Online]. Available: http://riker.unm.edu/DASH_new/pdf/ApplicationBriefs/Automated Road Network Extraction.PDF

[2] R. Nevatia and K. Babu, "Linear feature extraction and description," *Computer Graphics and Image Processing*, vol. 13, pp. 257–269, 1980.

[3] K. Treash and K. Amaratunga, "Automatic road detection in gray scale aerial images," *ASCE J. Computing in Civil Engineering*, vol. 14, no. 1, pp. 60–69, 2000.

[4] D. M. Mckeown, W. A. Harvey, and J. McDermott, "Rule-based interpretation of aerial imagery," *IEEE Trans. Pattern Analysis and Machine Intelligence*, vol. 7, no. 5, pp. 570–585, 1985.

[5] M. Zhu and P. Yeh, "Automatic road network detection on aerial photographs," in *Proc. Int. Conf. Computer Vision and Pattern Recognition*, Miami Beach, Florida, 1986, pp. 34–40.

[6] A. Gruen and H. Li, "Road extraction from aerial and satellite images by dynamic programming," *ISPRS J. Photogrammetry and Remote Sensing*, vol. 50, no. 4, pp. 11–21, 1995.

[7] D. Chaudhuri, A. Mishra, V. Gohri, and J. K. Sharma, "Automated detection of Tracks in Mountainous terrain using IRS-1C/1D images," in *Int. Conf. Computer Vision, Graphics and Image Processing, ICVGIP-2002*, 2002, pp. 394–399.

[8] R. Stoica, X. Descombes, and J. Zerubia, A Markov Process for Road Extraction in Remote Sensed Images, INRIA, Sophia Antipolis, France, Research Report: PR-3923, 2000 [Online]. Available: http://www.inria.fr/rrrt/rr-3923.html

[9] P. N. Anil and S. Natarajan, "Automatic road extraction from high resolution imagery based on statistical region merging and skeletonization," *Int. J. Engineering Science and Technology*, vol. 2, no. 3, pp. 165–171, 2010.

[10] U. Stilla, "Map-aided structural analysis of aerial images," *ISPRS J. Photogrammetric and Remote Sensing*, vol. 50, no. 4, pp. 3–9, 1995.

[11] X. Hu and V. Tao, "Automatic extraction of main road centerlines from high resolution satellite imagery using Hierarchical grouping," *Photogrammetric Engineering and Remote Sensing*, vol. 73, no. 9, pp. 1049–1056, 2007.

[12] J. B. Mena and J. A. Malpica, "Automatic method for road extraction in rural and semi-urban areas starting from high resolution satellite imagery," *Pattern Recognition Letters*, vol. 26, pp. 1201–1220, 2005.

[13] R. S. Wang, Y. Hu, and Zhang, "Extraction of road networks using pansharpened multi-spectral and panchromatic Quickbird images," *Geomatica*, vol. 59, pp. 263–273, 2005.

[14] S. M. Easa, H. Dong, and J. Li, "Use of satellite imagery for establishing road horizontal alignments," *J. Survey Engineering*, vol. 133, pp. 29–35, 2007.

[15] Y. Wang, Y. Tian, X. Tai, and L. Shu, "Extraction of main urban roads from high resolution satellite images by machine learning," in *Asian Conf. Computer Vision*, 2006, vol. 1, pp. 236–245.

[16] J. F. Yang and R. S. Wang, "Classified road detection from satellite images based on perceptual organization," *Int. J. Remote Sensing*, vol. 28, pp. 4653–4669, 2007.

[17] M. Mokhtarzade and M. J. ValadanZoej, "Road detection from high resolution satellite images using artificial neural networks," *Int. J. Appl. Earth Observ. Geoinform.*, vol. 9, pp. 32–40, 2007.

[18] F. F. Ahmadi, M. J. ValadonZoej, H. Ebadi, and M. Mokhtarzade, "Road extraction from high resolution satellite images using image processing algorithms and CAD-based environments facilities," *J. Applied Sciences*, vol. 8, no. 17, pp. 2975–2982, 2008.

[19] T. Tateyama, Z. Nakao, X. Y. Zeng, and Y. W. Chen, "Segmentation of high resolution satellite images by direction and morphological filters," in *Proc. 4th Int. Conf. Hybrid Intelligent Systems (HIS'04)*, 2004, IEEE Computer Society.

[20] D. Chaudhuri, C. A. Murthy, and B. B. Chaudhuri, "A modified metric to compute distance," *Pattern Recognition*, vol. 25, no. 7, pp. 667–677, 1992.

[21] D. Chaudhuri, A. Samal, A. Agrawal, Sanjay, A. Mishra, V. Gohri, and R. C. Agarwal, "A statistical based approach for automatic detection of ocean disturbance features from SAR images," *IEEE JSTARS*, 2012, 10.1109/JSTARS.2012.2186630.

[22] A. Rosenfeld and A. Kak, *Digital Picture Processing*. New York: Academic Press, 1982.

[23] M. Barzohar and D. B. Cooper, "Automatic finding of main roads in aerial images by using geometric stochastic models and estimation," *IEEE Trans. PAMI*, vol. 18, no. 7, pp. 707–721, 1996.

[24] S. Valero, J. Chanussot, J. A. Benediksttsson, H. Talbot, and B. Waske, "Advanced directional of the road network in very high resolution remote sensing images," *Pattern Recognition Letters*, vol. 31, no. 10, pp. 1120–1127, 2010.

[25] Q. Zhang and I. Coulorigner, "Benefit of the angular texture signature for the separation of parking lots and roads on high resolution multispectral imagery," *Pattern Recognition Letters*, vol. 27, pp. 937–946, 2006.

[26] B. Ahmed and M. F. Rahman, "Automatic road extractions from high resolution satellite imagery using road intersection model in urban areas," *Computer Engineering and Intelligent Systems*, vol. 2, no. 4, pp. 82–93, 2011.

[27] P. Doucette, P. Agouris, and A. Stefanidis, "Automated road extraction from high resolution multispectral imagery," *Photogrammetric Engineering and Remote Sensing*, vol. 70, no. 12, pp. 1405–1416, 2004.

[28] M. Ziems, M. Gerke, and C. Heipke, "Automatic road extraction from remote sensing imagery incorporating prior information and colour segmentation," *Photogrammetric Image Analysis PIA07*, vol. 36, International Archives of Photogrammetry, Remote Sensing and Spatial Information Sciences, pp. 141–147, 2007, U. Stilla *et al*, Eds..

[29] Imagine Objective User's Guide, ERDAS, pp. 13–27, 2009.

[30] C. Ünsalan and K. L. Boyer, "A system to detect houses and residential street networks in multispectral satellite images," *Computer Vision and Image Understanding*, vol. 98, no. 3, pp. 423–461, 2005.

[31] H. Mayer, S. Hinz, U. Bacher, and E. Baltsavias, "A test of automatic road extraction approaches," *Int. Archives Photogrammetry, Remote Sensing, and Spatial Information Sciences*, vol. 36-3, pp. 209–214, 2006.

D. Chaudhuri received the B.Sc. degree (with honors) in mathematics from Visva-Bharati University, Santiniketan, India, in 1985, the M.Sc. degree in applied mathematics from Jadavpur University, Kolkata, India, in 1987, and the Ph.D. degree in image processing and pattern recognition from Indian Statistical Institute, Kolkata, in 1994.

He is currently a Scientist with the Defence Electronics Applications Laboratory, Dehradun, India. He was a visiting Assistant Professor at the University of Nebraska in the Department of Computer Science and Engineering for 2003–2004 Session. His research interests include image processing, pattern recognition, computer vision, remote sensing and target detection from satellite imagery.

Dr. Chaudhuri is a reviewer and an Associate Editor of several international journals including *Pattern Recognition Letters* and the *International Journal of Computational Vision and Robotics*. He received the Technology Award from DRDO Science Forum, Mins. of Defence, Govt. of India in 2011. He has authored or coauthored over 45 papers in international journals and conferences in the area of image analysis.

N. K. Kushwaha received the B.Tech. degree in computer science and engineering from the Indian Institute of Technology, Kanpur, in 2009.

Presently he is a scientist at DEAL, DRDO, Dehradun, India. His fields of interest are image processing, pattern recognition, computer vision and remote sensing.

A. Samal received the B.Tech. degree in computer science from the Indian Institute of Technology, Kanpur, in 1983, and the Ph.D. in computer science from the University of Utah in 1988.

Since Fall 1988 he has been with the Department of Computer Science and Engineering at the University of Nebraska-Lincoln where he is currently an Associate Professor. His research interests are image understanding, document analysis, geospatial computing, and distributed computation. He has published over 70 papers in these areas in international journals and conferences.